Large-amplitude nonlinear normal modes of the discrete sine lattices

Valeri V. Smirnov* and Leonid I. Manevitch
Institute of Chemical Physics, RAS, 4 Kosygin Street, Moscow 119991, Russia
(Received 30 March 2016; revised manuscript received 25 November 2016; published 17 February 2017)

We present an analytical description of the large-amplitude stationary oscillations of the finite discrete system of harmonically coupled pendulums without any restrictions on their amplitudes (excluding a vicinity of π). Although this model has numerous applications in different fields of physics, it was studied earlier in the infinite limit only. The discrete chain with a finite length can be considered as a well analytical analog of the coarse-grain models of flexible polymers in the molecular dynamics simulations. The developed approach allows to find the dispersion relations for arbitrary amplitudes of the nonlinear normal modes. We emphasize that the long-wavelength approximation, which is described by well-known sine-Gordon equation, leads to an inadequate zone structure for the amplitudes of about $\pi/2$ even if the chain is long enough. An extremely complex zone structure at the large amplitudes corresponds to multiple resonances between nonlinear normal modes even with strongly different wave numbers. Due to the complexity of the dispersion relations the modes with shorter wavelengths may have smaller frequencies. The stability of the nonlinear normal modes under condition of the resonant interaction are discussed. It is shown that this interaction of the modes in the vicinity of the long wavelength edge of the spectrum leads to the localization of the oscillations. The thresholds of instability and localization are determined explicitly. The numerical simulation of the dynamics of a finite-length chain is in a good agreement with obtained analytical predictions.

DOI: 10.1103/PhysRevE.95.022212

I. INTRODUCTION

A wide class of physical models, the most known of which is the Frenkel-Kontorova (FK) model [1,2], is based on the dynamics of a pendulum. The physical applications of the FK model comprise a wide spectrum of the problems in the solid-state theory [1,3–8], the polymer physics [9], and certain biological processes like the DNA dynamics and denaturation [10] (more references may be found in Ref. [2]). The common peculiarity of the mentioned models is the presence of the periodic on-site potential, while the inter-particle interaction can be described by potentials with nonlinearities of different types. Periodic interatomic potentials arise, in particular, while dealing with magnetic systems, unzipping the DNA molecule and oscillations of the flexible crystalline polymers (see, e.g., Refs. [11–13], where the existence of the highly localized soliton-like solution has been proved in the framework of the sine-lattice model).

The lucky star of the Frenkel-Kontorova model is the existence of the integrable continuum limit of the respective equation of motion (sine-Gordon equation). Due to full integrability of the latter, its spectra of the nonlinear periodic and localized excitations have been studied in detail [14]. The continuum limit of the discrete model with the nonlinear periodic interatomic interaction leads to the same sine-Gordon equation with understandable restrictions on the wavelengths (accounting the discreteness effects in the framework of approach introduced by Rosenau [15] leads to the improvement of the long-wavelength approximation only).

The main goal of this article is the study of nonlinear normal modes (NNMs) of discrete lattice with nonlinear on-site and intersite interactions in the wide range of the oscillation amplitudes and wavelengths. We propose a new semi-inverse asymptotic approach, which was successfully implemented for two coupled pendulums in Ref. [16]. This approach allowed us to reveal an extremely complex zone structure at the large amplitudes that leads to multiple resonances between NNMs with strongly different wave numbers. In particular, the equations of motion obtained allow us to study the processes of the resonant interaction of the NNMs and to formulate the criterion of the modes' stability at different amplitudes and wave numbers of the oscillations. We also demonstrate that such a process as a localization of oscillations in the chain can be understood by considering the NNMs interaction in the framework of the asymptotic analysis.

II. THE MODEL

We consider a finite chain of coupled particles with periodic on-site and interparticle potentials; each of them is described by a harmonic function with, generally speaking, different periods. This system will be referred to as sine-lattice (SL), in contrast to the classic FK system. Keeping in mind the coincidence of the mathematical descriptions we will discuss all results in terms of coupled pendulums. The energy of such system may be written as follows:

$$H = \sum_{j=1}^{N} \left[\frac{1}{2} \left(\frac{dq_j}{dt} \right)^2 + \frac{\beta}{\alpha^2} \{1 - \cos[\alpha(q_{j+1} - q_j)]\} + (1 - \cos q_j) \right]; \quad j = 1, \ldots, N, \tag{1}$$

where q_j is the deviation of the jth pendulum, while β and α are the parameters that specify the rigidity and the period of interpendulum coupling. We use the periodic boundary conditions as the most appropriate for the analysis of the chain dynamics, i.e., we assume that $q_{N+1} = q_1$ and $q_0 = q_N$.

*vvs@polymer.chph.ras.ru

The respective equations of motion can be written as follows:

$$\frac{d^2q_j}{dt^2} - \frac{\beta}{\alpha}\{\sin[\alpha(q_{j+1} - q_j)] - \sin[\alpha(q_j - q_{j-1})]\} + \sin q_j = 0. \tag{2}$$

Introducing the complex variables given by

$$\Psi_j = \frac{1}{\sqrt{2}}\left(\frac{1}{\sqrt{\omega}}\frac{dq_j}{dt} + i\sqrt{\omega}q_j\right), \quad q_j = \frac{-i}{\sqrt{2\omega}}(\Psi_j - \Psi_j^*), \quad \frac{dq_j}{dt} = \sqrt{\frac{\omega}{2}}(\Psi_j + \Psi_j^*), \tag{3}$$

and substituting them in Eq. (2), one can rewrite Eq. (2) as

$$i\frac{d\Psi_j}{dt} + \frac{\omega}{2}(\Psi_j + cc), + \frac{1}{2\omega}\sum_{k=0}^{\infty}\frac{1}{(2k+1)!}\left(\frac{1}{2\omega}\right)^k\{(\Psi_j - cc)^{2k+1} - \beta\,\alpha^{2k}[(\Psi_{j+1} - \Psi_j - cc)^{2k+1} - (\Psi_j - \Psi_{j-1} - cc)^{2k+1}]\} = 0, \tag{4}$$

where the nonlinear terms in Eq. (2) are represented as the series of their arguments and abbreviation "cc" corresponds to the complex conjugates.

The semi-inverse resonance approach to the dynamic analysis without any restrictions on the oscillation amplitudes assumes that the considered system admits two timescales (fast and slow). In the framework of this approach corresponding small parameter as well as the frequency ω can be not presented in starting equations of motion Eq. (2) and they have to be determined later. In order to demonstrate these sentences one can start from the stationary solution of Eq. (4):

$$\Psi_j = \varphi_j e^{i\omega t}, \tag{5}$$

where $\varphi_j = \text{const}$. Inserting solution Eq. (5) into Eq. (4) with the further multiplying the latter on the factor $\exp(-i\omega t)$ and integrating over the period $2\pi/\omega$ leads to the transcendental equations for the envelope function φ_j:

$$-\frac{\omega}{2}\varphi_j + \frac{1}{\sqrt{2\omega}}J_1\left(\sqrt{\frac{2}{\omega}}|\varphi_j|\right)\frac{\varphi_j}{|\varphi_j|} - \frac{\beta}{\alpha\sqrt{2\omega}}\left[J_1\left(\alpha\sqrt{\frac{2}{\omega}}|\varphi_{j+1} - \varphi_j|\right)\frac{\varphi_{j+1} - \varphi_j}{|\varphi_{j+1} - \varphi_j|} - J_1\left(\alpha\sqrt{\frac{2}{\omega}}|\varphi_j - \varphi_{j-1}|\right)\frac{\varphi_j - \varphi_{j-1}}{|\varphi_j - \varphi_{j-1}|}\right] = 0, \tag{6}$$

where J_1 is the Bessel function of the first order.

It is easy to see that the procedure used above is somewhat similar to the harmonic balance method, which is widely used in the analysis of nonlinear oscillations [17].

In spite of the complexity of Eq. (6), one can directly check that the simple expression

$$\varphi_j = \sqrt{X}e^{-i\kappa j} \tag{7}$$

with the wave number $\kappa = 2\pi k/N$(k is an integer, $k \leqslant N/2$) satisfies it, if the frequency ω is the solution of the equation

$$-\frac{\omega}{2} + \frac{1}{\sqrt{2\omega X}}\left[2\frac{\beta}{\alpha}J_1\left(2\alpha\sqrt{\frac{2}{\omega}X}\sin\frac{\kappa}{2}\right)\sin\frac{\kappa}{2} + J_1\left(\sqrt{\frac{2}{\omega}X}\right)\right] = 0. \tag{8}$$

The latter equation is strongly simplified, if we use the relationship between the modulus of complex function X and the amplitude of oscillations Q, which results from definition Eq. (3) of complex variable Ψ:

$$X = \frac{\omega}{2}Q^2.$$

Taking into account this relationship leads to the expression for the NNMs' frequency of the oscillations with the given amplitude Q:

$$\omega^2 = \frac{2}{Q}\left[2\frac{\beta}{\alpha}J_1\left(2\,\alpha\,Q\sin\frac{\kappa}{2}\right)\sin\frac{\kappa}{2} + J_1(Q)\right]. \tag{9}$$

Prior to the analysis of eigenfrequencies Eq. (9) one should test the limiting case that corresponds to the oscillations of a single pendulum. Really, if the coupling parameter $\beta = 0$, Hamiltonian Eq. (1) describes a set of independent pendulums, the oscillation frequency of which depends on the amplitude Q. In such a case frequency Eq. (9) has the form:

$$\omega = \sqrt{\frac{2}{Q}J_1(Q)}. \tag{10}$$

Equation (10) can be compared with the exact oscillation frequency of pendulum:

$$\omega_e = \frac{\pi}{2K[\sin(Q/2)]}, \tag{11}$$

where K is the complete elliptic integral of the first kind.

One can see from Fig. 1 that the agreement for all amplitudes is excellent up to $Q \simeq 3\pi/4$ and turns out to be good enough even for $Q = 9\pi/10$.

In order to understand the origin of the frequencies divergence one should notice that Eq. (6) is the limiting stationary case of more commonly equation, which describes a slow evolution of the envelope function φ_J. The latter results from the interaction of the NNMs with close frequencies (it is an analog of the beating phenomenon in the linearized system). The specific time of this evolution is determined by the relative difference of the NNMs' frequencies. Until these values are small enough, the timescales may be separated well. However, when the oscillation amplitude Q approaches its maximum value π, the frequency rapidly diminishes and the difference mentioned above turns out to be nonsmall. So, the small parameter, which determines the timescale separation, is related with the gap between NNMs frequencies. We will demonstrate using this parameter at the analysis of the stability of the NNMs.

Equation (9) describes the NNM "zone" structure, i.e., the dispersion ratio for the SL model at the arbitrary oscillation amplitude (excluding the vicinity of the "rotation limit" $Q = \pi$).

One should note that because of model Eq. (1) leads to the discrete FK chain in the "long-wavelength" limit

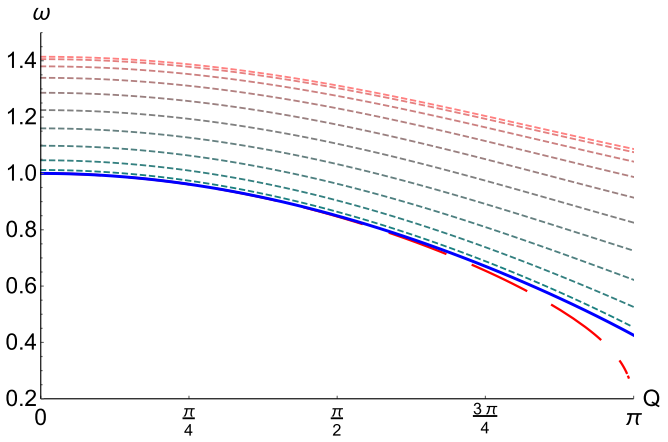

FIG. 1. Zone structure of the discrete FK chain with 20 particles (coupling parameter $\beta = 0.25$). Dashed curves correspond to the NNMs' frequencies Eq. (12); the low-frequency zone-bounding mode is shown by solid blue curve [see Eq. (10)]. Dashed red curve shows the exact frequency of pendulum oscillations according to Eq. (11).

$[\alpha(q_{j+1} - q_j) \ll 1]$, Eq. (9) has to describe the respective spectrum. Actually, considering the wave number κ as a small value, one can expand the Bessel function as a power series. The first term of Eq. (9) becomes $2\alpha Q \sin\kappa/2$ and the eigenfrequency is reduced as follows:

$$\omega^2 = 2\left[\frac{1}{Q}J_1(Q) + 2\beta\sin^2\frac{\kappa}{2}\right]. \tag{12}$$

Figure 1 shows the zone structure for the FK chain with 20 particles under periodic boundary conditions.

The low-frequency mode, which bounds the zone, corresponds to the uniform oscillations of the chain or to the oscillations of the single pendulum Eq. (10), while the high-frequency bounding mode corresponds to the out-of-phase pendulum oscillations ("π" mode). One can see that frequency Eq. (12) is the monotonically increasing function of the wave number κ, but the difference $\Delta\omega^2 = \omega^2(\kappa = \pi) - \omega^2(\kappa = 0)$ does not depend on the amplitude of oscillations.

Figure 2 shows zone structure for the harmonically coupled pendulums.

The comparison of Figs. 1 and 2 shows a cardinal distinction between them. First, the width of the SL zone depends on the amplitude of oscillations. It is more important that the dispersion relation at a fixed amplitude $Q \geqslant \pi/2$ (the threshold value depends on the parameters α and β) is a nonmonotonic function of the wave number. As a result, the frequency of the zone bounding π mode turns out to be smaller than the frequency of the uniform mode for large Q. In such a case the multiple resonances occur in the vicinity of right edge of the spectrum, and their existence is defined by nonmonotonic character of the dispersion relation rather than by the length of the chain. Figure 3 shows the dispersion relation for SL chain with 20 pendulums and the oscillation amplitude $Q = \pi/10$ in comparison with the same for $Q = 9\pi/10$.

The structure of the NNMs zone for the SL chain has been checked by the direct numerical integration of Eq. (2).

Figure 4 allows to compare the positions of the zone bounding modes and some intermediate ones. One can see that

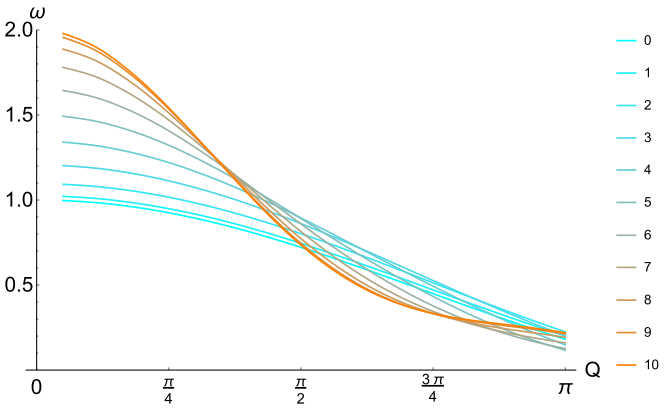

FIG. 2. The zone structure for the SL chain with 20 pendulums under periodic boundary conditions. Light blue and light brown curves correspond to the zone bounding uniform and π modes, respectively. The coupling parameters $\beta = 0.25, \alpha = 1.2$. The numbers in the figure legend show the mode's number.

the mutual positions of the modes correspond to the dispersion relations that are shown in Fig. 3.

Due to nonmonotonic behavior of the dispersion relations at the large amplitudes (Fig. 3), a multitude of the resonances can exist for both the NNMs with the nearby wave numbers and for the modes, the wave numbers of which differ significantly. Moreover, an almost flat dispersion relation can be obtained for the certain combination of the lattice parameters α and β. In such a case the thermoconductivity of the system decreases essentially due to the effective phonon scattering [18].

An initial excitation of general nature *a priori* contains some combination of the modes with different amplitudes. In contrast to a linear system, where any interaction between normal modes is absent, the NNMs in the essentially nonlinear systems can interact efficiently if the resonant conditions occur [19]. Therefore, the problem of internal resonances is very important for study of the dynamics of the sine-lattice.

Figures 5 show the "map" of resonantly interacting modes for two amplitudes of the oscillations: $Q = 3\pi/10$ and

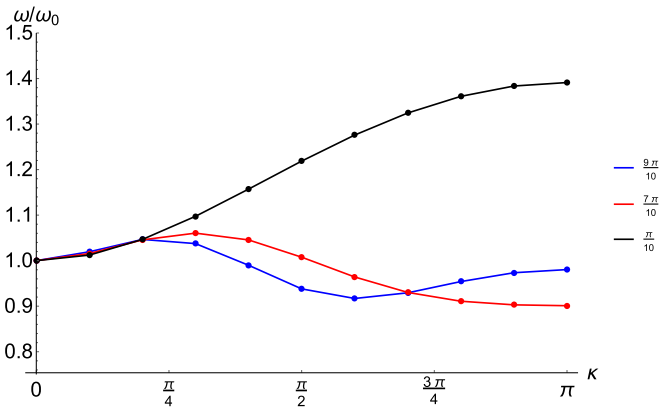

FIG. 3. The comparison of the dispersion relations for the SL chain with 20 pendulums at the different oscillation amplitudes: black, red and blue points correspond to the amplitudes $Q = \pi/10$, $Q = 7\pi/10$, and $Q = 9\pi/10$, respectively. The relative frequencies ω/ω_0 (ω_0 is the frequency of the uniform modes) are shown. The potential parameters: $\beta = 0.25$, $\alpha = 1.2$.

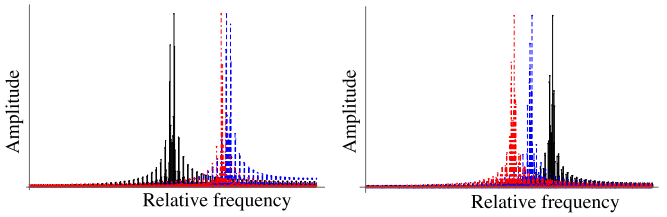

FIG. 4. Fourier spectra of the oscillations of SL chain with eight pendulums. Left panel shows the frequencies of the normal mode with $\kappa = 0, 3\pi/4, \pi$ (solid black, dot-dashed red, and dashed blue lines, respectively) at the amplitude $Q = \pi/10$. Right panel shows the same as left one at the amplitude $Q = 9\pi/10$. The potential parameters: $\beta = 0.25, \alpha = 1.2$

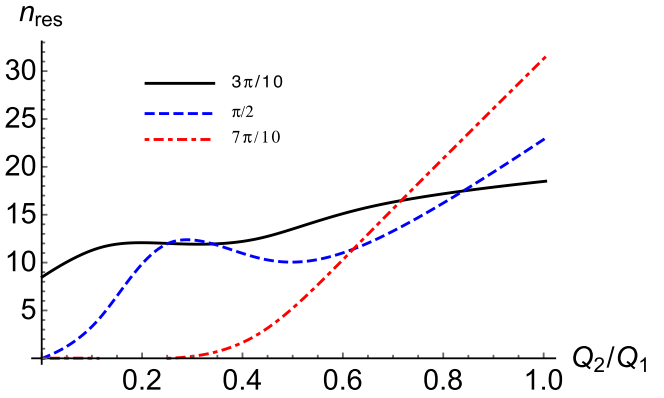

FIG. 6. The number of resonances vs. partial amplitude ratio for total oscilllation amplitudes $Q = 3\pi/10, \pi/2, 7\pi/10$

$Q = 7\pi/10$. The Figs. 5(a)–5(f) differ in the partial amplitudes of interacting modes Q_1 and Q_2 at the constant sum of them: $Q = Q_1 + Q_2$.

One can see that for a small amplitude Q, the resonantly interacting modes have the close numbers: $k_1 \simeq k_2$ for any ratios of the partial amplitudes of the modes (Q_1 and Q_2 [see Fig. 5(i)]. In contrast to that, the oscillations with a large amplitude [Fig. 5(iii)] do not contain the resonantly interacting modes for small values Q_2 and include the multitude of resonant modes in the short wavelength domain of the spectrum. Figure 6 shows the number of resonances as a function of the ratio Q_2/Q_1 for three values of the oscillation amplitude: $Q = 3/\pi/10, \pi/2, 7\pi/10$.

There are at least two reasons for the importance of the NNMs interactions. As it was shown early, the resonant interaction of the NNMs leads to the localization effect (the capture of the energy of oscillations in some domain of the chain) [20–22]. The necessary condition of such localization is the instability of one of interacting modes [23].

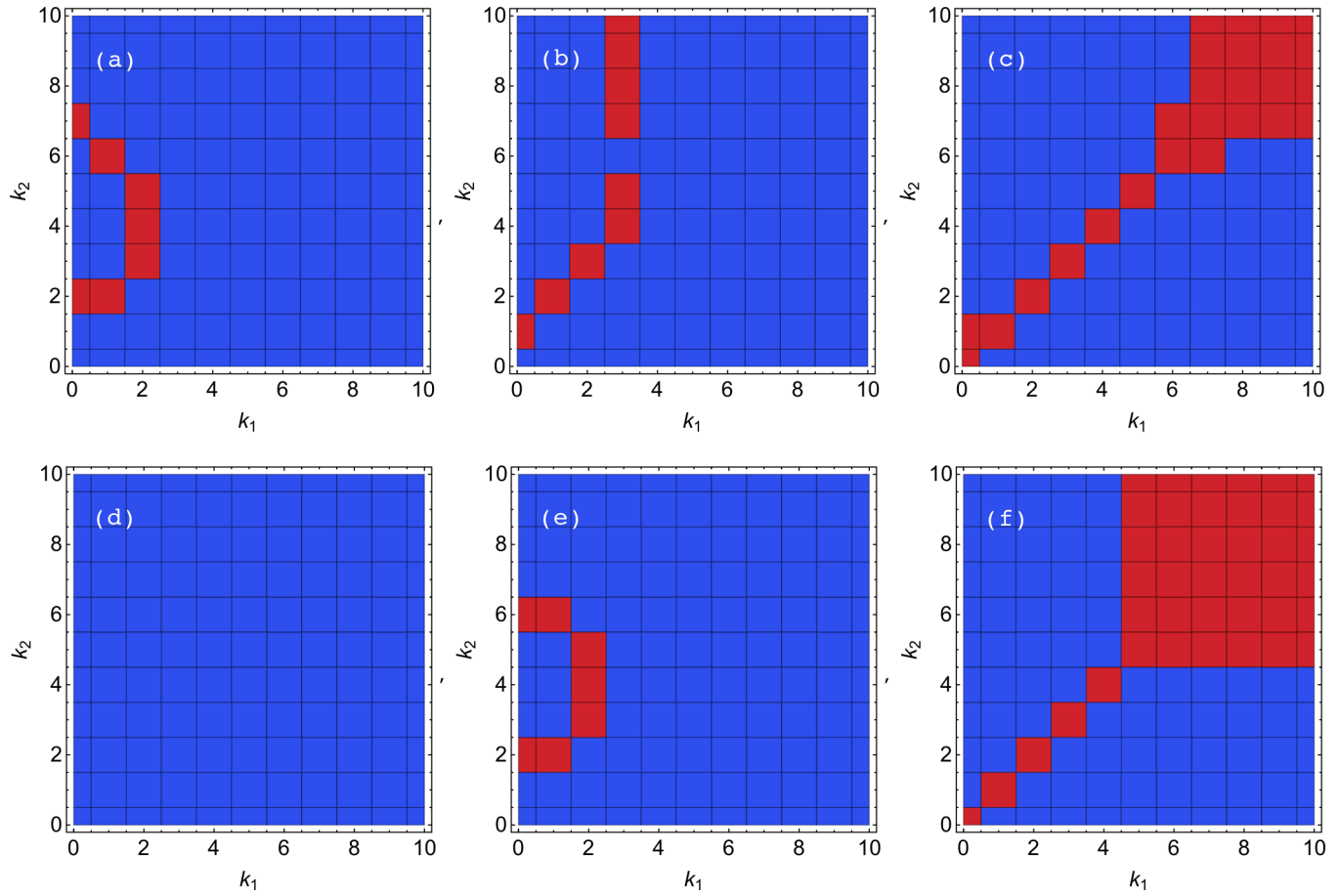

FIG. 5. Maps of resonances for two values of oscillation amplitudes: $Q = \pi/2$ (a–c) and $Q = 7\pi/10$ (d–f). k_1 and k_2 are the modes' numbers. The panels (a–c) and (d–e) differ in the partial amplitudes of the modes Q_1 and Q_2. The red squares correspond to the modes the frequencies of which differ not more than 5%.

The second reason arises from the occurrence of the chaotic regimes of the oscillations under conditions of internal nonlinear resonances [19,24–26]. As it was mentioned above, the continuum approximation of Eq. (2) leads to the well-known sine-Gordon equation, which corresponds to the integrable system and does not allow any chaotic behavior. In contrast with the latter the considered system is not an integrable one. Taking into account the multitude of internal resonances, one should expect the existence of the chaotic trajectories in the phase space of the system. The chaotic trajectories arise inside the stochastic layer nearby the separatrix passing via the unstable singularity, which is formed when one of resonantly interacting modes loses its stability [27].

Therefore, the stability of the NNMs is one of the key problems of the dynamics of the system under consideration.

In order to analyze the stability of the NNMs we will use the nonstationary extension of Eq. (6). Let us assume that the initial conditions contain alongside with considered NNM (stationary solution) a small perturbation corresponding to mode with different wave number:

$$\varphi_j = \sqrt{X}(1+\varepsilon\chi_j)e^{i\kappa j} = \varphi_{j,0} + \varepsilon\chi_j, \tag{13}$$

where $\varphi_{j,0}$ is the solution of stationary Eq. (6). In such a case one should wait that Eq. (6) is not satisfied. It is easy to understand that this envelope will have a large timescale (in the comparison with the period of the carrier $2\pi/\omega$) if the frequencies of the interacting modes turn out to be close. The short discussion of the time separation procedure is presented in the Appendix. As a result the time-dependent equations can be written as follows:

$$\begin{aligned} i\frac{\partial\varphi_j}{\partial\tau_1} - \frac{\omega}{2}\varphi_j + \frac{1}{\sqrt{2\omega}}J_1\left(\sqrt{\frac{2}{\omega}}\,|\varphi_j|\right)\frac{\varphi_j}{|\varphi_j|} \\ - \frac{\beta}{\alpha\sqrt{2\omega}}\left[J_1\left(\alpha\sqrt{\frac{2}{\omega}}\,|\varphi_{j+1}-\varphi_j|\right)\frac{\varphi_{j+1}-\varphi_j}{|\varphi_{j+1}-\varphi_j|}\right. \\ \left. - J_1\left(\alpha\sqrt{\frac{2}{\omega}}\,|\varphi_j-\varphi_{j-1}|\right)\frac{\varphi_j-\varphi_{j-1}}{|\varphi_j-\varphi_{j-1}|}\right] = 0. \end{aligned} \tag{14}$$

Assuming the function Eq. (13) in the form

$$\begin{aligned} \varphi_j &= \sqrt{X}[e^{i\kappa j} + s(\tau_1)e^{i\nu j}] \\ &= \sqrt{X}\{e^{i\kappa j} + [u(\tau_1)+v(\tau_1)]e^{i\nu j}\}, \end{aligned} \tag{15}$$

where u and v are the real functions of the slow time τ_1, one can analyze the effect of the mode with wave number ν on the NNM with wave number κ. Expanding Eq. (14) in the vicinity of the NNM φ and keeping the perturbation of first order only, one can obtain the equation for the real part of the function s as follows:

$$\frac{\partial^2 u}{\partial\tau_1^2} + \Lambda u = 0, \tag{16}$$

where the parameter Λ is

$$\begin{aligned} \Lambda = \frac{1}{8\omega\sin\frac{\kappa}{2}}\left[2\frac{\beta}{\alpha}J_1\left(2\alpha Q\sin\frac{\kappa}{2}\right)(\cos\kappa-\cos\nu) - 4\beta Q J_2\left(2\alpha Q\sin\frac{\kappa}{2}\right)\sin^2\frac{\nu}{2}\sin\frac{\kappa}{2} - Q J_2(Q)\right]^2 \\ - \frac{Q^2\sin\frac{\kappa}{2}}{8\omega}\left[2\beta(\cos(\kappa-\nu)-\cos\kappa)J_2\left(2Q\alpha\sin\frac{\kappa}{2}\right) + J_2(Q)\right]^2. \end{aligned} \tag{17}$$

The stability of the NNM is determined by the sign of the parameter Λ. If $\Lambda > 0$, the perturbation remains a small, but it increases if $\Lambda < 0$. The parameter Λ depends on the lattice parameters α and β as well as on the amplitude Q. Let us determine the coupling parameter β at the threshold of stability. Solving the equation

$$\Lambda = 0$$

with respect to β, one can obtain its critical value as follows:

$$\beta_{\text{ins}} = \frac{\alpha Q J_2(Q)\sin\frac{\kappa}{2}}{J_1\left(2Q\alpha\sin\frac{\kappa}{2}\right)(\cos\kappa-\cos\nu) - 4\alpha Q J_2\left(2Q\alpha\sin\frac{\kappa}{2}\right)\sin^2\frac{\kappa}{2}\sin\frac{\nu}{2}\cos\left[\frac{1}{2}(\kappa-\nu)\right]}. \tag{18}$$

As it was shown earlier [20,22,28], the stability of the zone-bounding mode with $\kappa = 0$ is important for the localization of the oscillations. Namely, the lost of the stability of this mode is the first step to stationary nonuniform distribution of the oscillation energy along the chain. Assuming $\kappa = 0$ and $\nu = 2\pi/N$, one can obtain the instability threshold for the zone-bonding mode as follows:

$$\beta_{\text{ins}} = \frac{1}{2}\frac{J_2(Q)}{\sin^2(\pi/N)}, \tag{19}$$

which correlates well with the estimation of analogous instability threshold for the Frenkel-Kontorova chain $\beta = (3Q/16\pi)^2N^2$ in the small-amplitude limit [22].

The "instability map" of the zone-bounding mode for the chain with $N = 20$ is shown in Fig. 7. One can see that the instability threshold increases significantly while the oscillation amplitude grows. It seems from the physical viewpoint that a large coupling parameter has no sense. It means that the large-amplitude uniform oscillations will be unstable in the majority of the physical systems.

We will not consider the stability of other resonantly interacting modes because due to the simpleness of Eq. (18) this problem can be analyzed for any physical systems.

However, the lost of stability of the zone-bounding mode does not imply the creation of the localized oscillation in the chain. There is the second bifurcation after that the processes

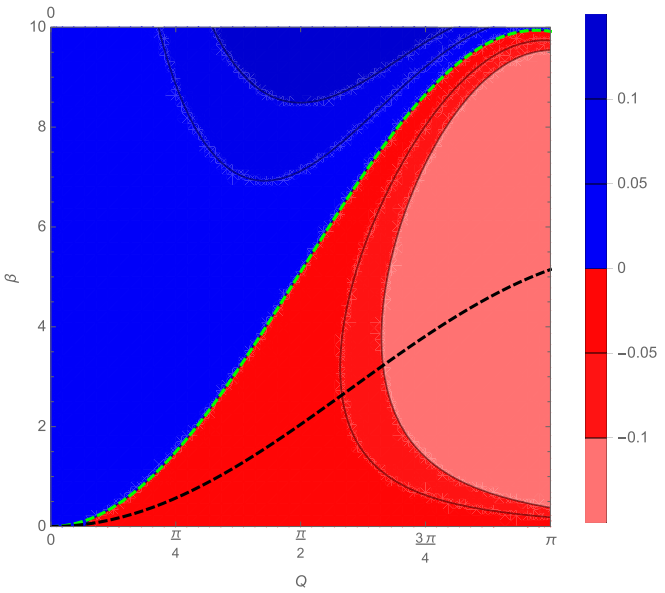

FIG. 7. Stability map of the zone-bounding mode with wave number $\kappa = 0$ in the coordinates (Q, β). The blue and red domains correspond to the stability and instability of the mode. The figure legend shows the specific values of the parameter Λ. The boundary between domains is marked by bright dashed line. The threshold of the localization is shown as the black dashed curve (see text). The length of chain is equal to 20 and parameter $\alpha = 1.25$.

of the energy redistribution are forbidden [20]. This bifurcation occurs when the energy of the unstable mode turns out to be equal the energy of the mixed state of the stable and unstable modes. Such a state corresponds to the limiting phase trajectory (LPT), which describes the nonstationary dynamics of the chain with the extremely large energy exchange between some parts of the system. The motion of the pendula inside this parts are closed to the coherent oscillations while the dynamics of the pendula in different parts differ essentially. The process of the energy exchange between these parts (clusters or coherent domains) of the system is similar to the beating in the system of two weakly coupled oscillators while the energy localization is analogous of the energy capture of one of them.

In order to estimate the localization threshold one should use the hamiltonian corresponding to Eq. (14):

$$H_a = \sum_{j=1}^{N}\Big[-\frac{\omega}{2}|\varphi_j|^2 + \frac{\beta}{\alpha^2}\Big(1 - J_0(\alpha\sqrt{\frac{2}{\omega}}|\varphi_{j+1} - \varphi_j|)\Big) + \Big(1 - J_0\Big(\sqrt{\frac{2}{\omega}}|\varphi_j|\Big)\Big)\Big]. \tag{20}$$

As it was mentioned above, the regimes with the energy localization occurs when the NNMs with wave number $\kappa = 0$ and $\kappa = 2\pi/N$ interact resonantly. Setting energy Eq. (20) of the zone-bounding mode solution ($\varphi_j = \text{const}$) equal to the energy of the mode mixture ($\varphi_j \sim 1 + \exp(i2\pi/N)$), one can get the localization threshold of the coupling parameter as follows:

$$\beta_{\text{loc}} = \frac{\alpha^2}{4}\frac{4J_0^2(Q/2) - 4J_0(Q) - QJ_1(Q)}{1 - J_0[\alpha Q \sin(\pi/N)]}. \tag{21}$$

The black dashed curve in Fig. 7 shows the value of the localization threshold Eq. (21) for the chain with 20 pendula and parameter $\alpha = 1.25$. One can see that the localization threshold β_{loc} grows essentially slower than the value β_{ins}; however, it reaches a large enough values for the large oscillation amplitudes $Q \geqslant \pi/2$. On the other side one should notice that the small-amplitude expansion of Eq. (21) shows that the value $\beta \sin^2 \pi/N$ turns out to be small, if the length of the chain is large enough. It correlates strongly with the assumptions about the resonance of the considered modes, because splitting between them is proportional this value.

Figures 8(a)–8(c) show the energy distribution along the chain for different values of the coupling parameter β—before and after threshold value β_{loc}. These figure were obtained by the direct numerical integration of the equations of motion which correspond to the initial Hamiltonian Eq. (1) under the periodic boundary conditions. The period of the zone-bounding mode at the amplitude $Q = \pi/2$ is $T = 2\pi/\omega \simeq 7.4$ time units.

Figure 8(a) shows the periodic energy redistribution along the chain before the localization ($\beta = 1.76$): the bright and dark areas change their location with the period, which is essentially larger than the oscillation one. Figure 8(b)

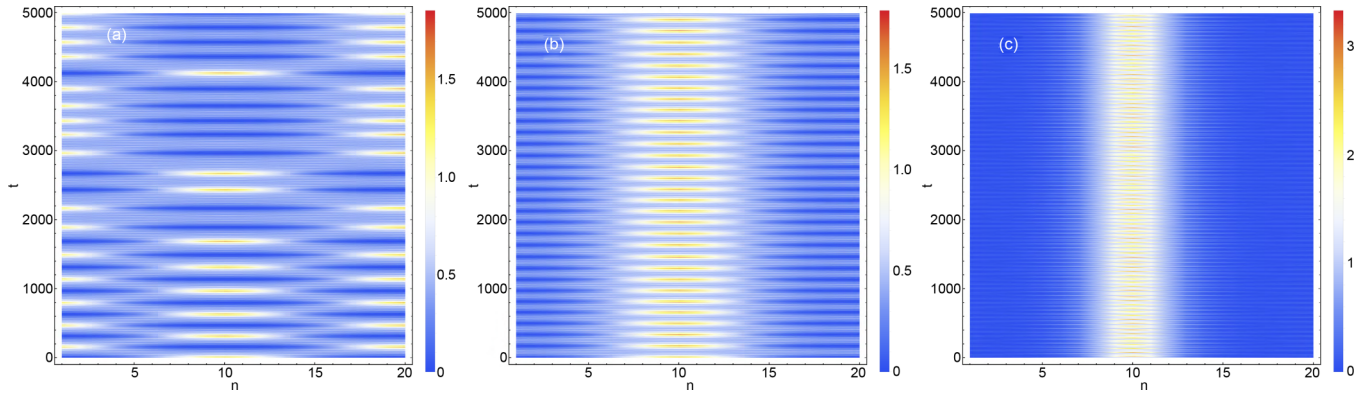

FIG. 8. Energy distribution along the chain with 20 pendula for three values of the coupling parameter β: 1.76 (a), 1.75 (c), and 1.00 (c). Parameter $\alpha = 1.25$. Amplitude of oscillation $Q = \pi/2$. The figure legends show the energy value in the dimensionless units.

demonstrates the energy distribution at the coupling parameter $\beta = 1.75$, which is under previous value less than 1% . One can see that the main part of the energy is localized near the center of the chain. Finally, Fig. 8(c) shows the well localized oscillations at the coupling parameter $\beta = 1.00 \ll \beta_{\text{loc}}$. One should notice that the estimation of the localization threshold with Eq. (21) for the used parameters gives the value $\beta = 2.044$, while as it can be seen from Fig. 8(b) shows the the localization occurs at $\beta \simeq 1.755$. The difference between the numerical result and the analytical estimation is approximately 15%.

III. CONCLUSIONS

The study of normal modes of the SLs revealed that the high-amplitude oscillations of harmonically coupled pendulums possess nontrivial dispersion relation, when the normal modes with higher wave numbers correspond to smaller oscillation frequencies. This peculiarity of the SL is a consequence of competition of the intersite and on-site parts of the potentials. Actually, the nonmonotonic behavior of the intersite potential can lead to decreasing the contribution of the dispersion term in Eq. (6). The competition between on-site and intersite interactions occurs when the difference of the displacements between neighbor pendulums turns out to be large enough, i.e., for the short wavelength oscillations. In the continuum limit, the dispersion terms of Eq. (6) are reduced to the second derivation of variable φ. As a result, the dispersion terms do not depend on the amplitude anymore. This correlates with that the continuum equation can be used for description of the long wavelength range only.

The analytical semi-inverse approach with multiple scale procedure turns out to be efficient for the investigation of different types of nonlinear lattices. This approach requires us to determine the value of the small parameter, which allows us to separate the timescales.

A natural small parameter in the problem is the value of the gap between the frequencies of adjacent NNMs. In spite of not having a small parameter in the initial equations, we are able to single it out in the process of solution. In particular, the equations in terms of the complex amplitudes, which are similar to Eq. (6), allow us to study the nonlinear normal mode interaction (see, e.g., Refs. [20–22,29]) that opens a wide possibilities for the analysis of nonlinear systems in various fields of physics. For example, the lattices with a wide class of nonlinear on-site and intersite potentials may be analyzed in the framework of this method. On the other side, this method allows us to analyze weakly coupled small systems, providing the coupling parameter is sufficiently small [16].

We have shown that using the asymptotic time-dependent evolution Eq. (14) with Hamiltonian Eq. (20) is a useful approach to study the resonant interactions of the NNMs in a wide range of the amplitudes and wave numbers. In particular, this approach allows us to determine the domains of NNMs' stability and to estimate the threshold of the energy localization analytically.

ACKNOWLEDGMENT

The work was supported by Russian Science Foundation (Grant No. 16-13-10302).

APPENDIX: TIMESCALE SEPARATION

In the framework of the multiscale method the "fast" and "slow" times are determined by the rules

$$\tau_0 = t, \quad \tau_1 = \varepsilon\tau_0,$$

and the derivative with respect to the time is

$$\frac{d}{dt} = \frac{\partial}{\partial\tau_0} + \varepsilon\frac{\partial}{\partial\tau_1}.$$

Let us rewrite Eq. (6) as follows:

$$\frac{\partial\varphi_j}{\partial\tau_0} + \varepsilon\frac{\partial\varphi_j}{\partial\tau_1} - \frac{\omega}{2}\varphi_j + F(\varphi_j) = 0, \tag{A1}$$

where

$$\begin{aligned} F(\varphi) = {} & \frac{1}{\sqrt{2\omega}} J_1\left(\sqrt{\frac{2}{\omega}}\,|\varphi_j|\right)\frac{\varphi_j}{|\varphi_j|} \\ & - \frac{\beta}{\alpha\sqrt{2\omega}}\left[J_1\left(\alpha\sqrt{\frac{2}{\omega}}\,|\varphi_{j+1}-\varphi_j|\right)\frac{\varphi_{j+1}-\varphi_j}{|\varphi_{j+1}-\varphi_j|}\right. \\ & \left. - J_1\left(\alpha\sqrt{\frac{2}{\omega}}\,|\varphi_j-\varphi_{j-1}|\right)\frac{\varphi_j-\varphi_{j-1}}{|\varphi_j-\varphi_{j-1}|}\right]. \end{aligned}$$

Let us consider the solution in the form $\varphi_j = \varphi_{j,0} + \varepsilon\chi_j$, where $\varphi_{j,0}$ satisfy Eq. (6) and ε is a small parameter. Taking into account that $\varphi_{j,0} = \text{const}$, one can write Eq. (A1) as follows:

$$\varepsilon\frac{\partial\chi_j}{\partial\tau_0} + \varepsilon^2\frac{\partial\chi_j}{\partial\tau_1} - \frac{\omega}{2}(\varphi_{j,0}+\varepsilon\chi_j) + F(\varphi_{j,0}+\varepsilon\chi_j) = 0. \tag{A2}$$

One can consider this equation from the viewpoint of the order of small parameter ε:

$$\begin{aligned} & \varepsilon\frac{\partial\chi_j}{\partial\tau_0} + \varepsilon^2\frac{\partial\chi_j}{\partial\tau_1} - \frac{\omega}{2}\varphi_{j,0} + F(\varphi_{j,0}) \\ & \quad - \varepsilon\left[\frac{\omega}{2} - \left(\frac{\partial}{\partial x}F(x)\right)_{x=\varphi_{j,0}}\right]\chi_j = 0. \end{aligned} \tag{A3}$$

Taking into account Eq. (6), one can get

$$\begin{aligned} & \varepsilon\frac{\partial\chi_j}{\partial\tau_0} + \varepsilon^2\frac{\partial\chi_j}{\partial\tau_1} - \varepsilon\left(\frac{\omega}{2} - \left(\frac{\partial}{\partial x}F(x)\right)_{x=\varphi_{j,0}}\right)\chi_j \\ & = \varepsilon\frac{\partial\chi_j}{\partial\tau_0} + \varepsilon^2\frac{\partial\chi_j}{\partial\tau_1} - \varepsilon\left[\frac{\partial}{\partial x}\left(\frac{\omega}{2}x - F(x)\right)\right]_{x=\varphi_{j,0}}\chi_j = 0. \end{aligned} \tag{A4}$$

So, if the last term in Eq. (A4) corresponds to a small value of order ε, one can separate the different orders of the small parameter ε:

$$\begin{aligned} & \varepsilon : \frac{\partial\chi_j}{\partial\tau_0} = 0, \\ & \varepsilon^2 : \frac{\partial\chi_j}{\partial\tau_1} - \frac{1}{\varepsilon}\left[\frac{\partial}{\partial x}\left(\frac{\omega}{2}x - F(x)\right)\right]_{x=\varphi_{j,0}}\chi_j = 0. \end{aligned} \tag{A5}$$

One should notice that the term in the square brackets has to be proportional to the relative difference of the modes' frequencies $\Delta\omega/\omega$ and the small parameter ε can be estimated

as follows:

$$\varepsilon \simeq \Delta\omega/\omega.$$

Because the stationary solution $\varphi_{j,0}$ does not depend on the time, the nonlinear evolution equation may be written as Eq. (14).

[1] Y. Frenkel and T. Kontorova, Phys. Z. Sowietunion **13**, 1 (1938).
[2] O. M. Braun and Y. S. Kivshar, *The Frenkel-Kontorova Model* (Springer-Verlag, Berlin/Heidelberg, 2004), p. 333.
[3] H. R. Paneth, Phys. Rev. **80**, 708 (1950).
[4] W. Doring, Z. Naturf. **3a**, 373 (1948).
[5] U. Enz, Helv. Phys. Acta **37**, 245 (1964).
[6] M. Suezawa and K. Sumino, Phys. Status Solidi A **36**, 263 (1976).
[7] I. F. Lyuksyutov, A. G. Naumovets, and V. L. Pokrovsky, *Two-Dimensional Crystals* (Academic Press, Boston, 1992).
[8] S. Pnevmatikos, Phys. Rev. Lett. **60**, 1534 (1988).
[9] E. A. Zubova, J. Exp. Theor. Phys. **93**, 895 (2001).
[10] S. Yomosa, Phys. Rev. A **27**, 2120 (1983).
[11] S. Takeno and S. Homma, J. Phys. Soc. Jpn. **55**, 65 (1986).
[12] S. Takeno and M. Peyrard, Physica D **92**, 140 (1996).
[13] S. Takeno and M. Peyrard, Phys. Rev. E **55**, 1922 (1997).
[14] S. Novikov, S. Manakov, L. Pitaevskii, and V. Zakharov, *Theory of Solitons: The Inverse Scattering Method*, Monographs in Contemporary Mathematics (Springer, New York, 1984), p. 276.
[15] P. Rosenau, Phys. Lett. A **118**, 222 (1986).
[16] L. I. Manevitch and F. Romeo, Europhys. Lett. **112**, 30005 (2015).
[17] R. E. Mickens, *Truly Nonlinear Oscillators: An Introduction to Harmonic Balance, Parameter Expansion, Iteration, and Averaging Methods* (World Scientific Publishing, Singapore, 2010).
[18] H. Han, L. Feng, S. Xiong, T. Shiga, J. Shiomi, S. Volz, and Y. A. Kosevich, Phys. Rev. B **94**, 054306 (2016).
[19] B. V. Chirikov and G. M. Zaslavsky, Sov. Phys. Usp. **14**, 549 (1972).
[20] L. I. Manevitch and V. V. Smirnov, Phys. Rev. E **82**, 036602 (2010).
[21] L. I. Manevitch and V. V. Smirnov, Doklady Physics **55**, 324 (2010).
[22] V. V. Smirnov and L. I. Manevitch, Acoust. Phys. **57**, 271 (2011).
[23] T. Dauxois and M. Peyrard, Phys. Rev. Lett. **70**, 3935 (1993).
[24] R. Z. Sagdeev, D. A. Usikov, and G. M. Zaslavsky, *Nonlinear Physics: From the Pendulum to Turbulence and Chaos* (Harwood Academic Publishing, New York, 1988), p. 315.
[25] A. I. Neishtadt, J. Appl. Math. Mech. **39**, 594 (1975).
[26] V. I. Arnold, V. V. Kozlov, and A. I. Neishtadt, in *Mathematical Aspects of Classical and Celestial Mechanics*, 3rd ed., Encyclopaedia Math. Sci., Vol. 3 (Springer, Berlin, 2006).
[27] G. M. Zaslavsky, *Physics of Chaos in Hamiltonian Dynamics* (Imperial College Press, London, 1998), p. 350.
[28] M. Peyrard and A. R. Bishop, Phys. Rev. Lett. **62**, 2755 (1989).
[29] V. V. Smirnov, D. S. Shepelev, and L. I. Manevitch, Phys. Rev. Lett. **113**, 135502 (2014).